RSC Advances

PAPER

View Article Online
View Journal | View Issue

Cite this: *RSC Adv.*, 2022, **12**, 19965

Slippage- and load-induced changes in the crystalline orientation of oligo(3-methoxythiophene) powder to develop a gold-tone luster†

Satoya Sugiura,[a] Terumasa Mitogawa,[a] Kota Saito,[a] Rihito Tamura,[a] Satoru Tsukada,[a] Takahiko Horiuchi[b] and Katsuyoshi Hoshino *[a]

The achievement of molecular orientation control by rubbing and pressing poly(3-alkylthiophene)s is a powerful technique to improve the performance of organic electronic devices. We report here that the rubbing and pressing of blackish-brown 3-methoxythiophene oligomer powders yield layer and tablet samples with gold tones, respectively. Specular reflectivity, colorimetric, and X-ray diffraction measurements reveal that this gold tone is caused by an increase in the ratio of edge-on lamellar crystallites to face-on ones, which is promoted by rubbing/pressing. In contrast to the 3-alkylthiophene polymer, which develops a dominant face-on lamellar structure, rubbing of the 3-methoxythiophene oligomer increases the relative amount of edge-on lamellar crystallites to face-on lamellar ones. Furthermore, gold tone development in the tablet samples is limited to the near-surface area, despite the fact that pressure is also applied to the tablet bulk. These specific chemical events are explained by considering the repulsive interactions between the 3-methoxythiophene backbone and the functional groups on the surface of the substrate employed during the rubbing/pressing processes. Despite the lower applied pressure, gold tone development by rubbing is accompanied by a higher reflective property than by pressing because of the formation of larger relative amounts and sizes of edge-on lamellar crystallites, which are responsible for the gold tone.

Received 8th June 2022
Accepted 4th July 2022

DOI: 10.1039/d2ra03538c

rsc.li/rsc-advances

1. Introduction

Over the last few decades, metal-free organic solids that exhibit gold, silver, or copper-like lusters have been discovered. These organic materials have attracted considerable attention because they have the potential to solve various issues associated with paints that contain metal flake pigments.[1,2] Among these organic materials, the method by which the metallic luster is developed differs depending on the chemical properties of the material. Such methods include crystallization,[3–8] solidification by filtration,[9–12] electrochemical polymerization,[13–16] and solution application.[17–23] However, the design of a novel and more facile method for the development of metallic lusters could promote the application of the corresponding organic materials in the field of decoration, while also expanding their range of uses.

The molecular orientation of semiconducting polymers (SCPs) such as polyalkylthiophenes[24,25] has been achieved using shear forces, such as those resulting from the mechanical rubbing of SCP films[26–30] and the friction transfer of polymers onto a substrate.[31–33] Mechanical rubbing typically involves the use of a cloth-covered rubbing cylinder that rotates at a steady speed and pressure to achieve orientation within the polymer films, while during friction transfer, the polymer powder is pressed at a high pressure to form a pellet, which is then slid onto a hot substrate at a constant speed to achieve polymer transfer onto the substrate. These methods achieve orientation of polymer chains in the direction of rubbing or friction, and it is well known that a correlation exists between the electronic properties and orientations of SCPs films. For example, in the case of poly(3-hexylthiophene) (P3HT) films, both edge-on lamellar crystallites (*i.e.*, where the thiophene rings are normal to the substrate and the π–π stacking direction lies in-plane) and face-on lamellar crystallites (*i.e.*, where the thiophene rings are parallel to the substrate and the π–π stacking direction is normal to the substrate) exist in the film. The former and latter orientations have been shown to favor the transport of charge carriers in the in-plane and film-thickness

[a]*Department of Materials Science, Graduate School of Engineering, Chiba University, 1-33 Yayoi-cho, Inage-ku, Chiba 263-8522, Japan. E-mail: k_hoshino@faculty.chiba-u.jp*

[b]*Department of Imaging Sciences, Graduate School of Engineering, Chiba University, 1-33 Yayoi-cho, Inage-ku, Chiba 263-8522, Japan*

† Electronic supplementary information (ESI) available: Photograph of O3MeOT milled in a mortar; surface morphology observation for O3MeOT tablets; variable-angle spectral reflectance measurements. See https://doi.org/10.1039/d2ra03538c

directions, respectively.[34] More specifically, rubbing the film surface parallel to the in-plane direction promotes face-on orientation formation and enhances the charge carrier mobility in the film thickness direction. The above rubbing and friction-induced orientation approaches have therefore been employed to improve the device performances of organic field-effect transistors,[35] polymerized light-emitting diodes,[32] organic thin-film solar cells,[28] and thermoelectric materials,[36] among others.

Thus, we herein report the use of a 3-methoxythiophene oligomer (a blackish-brown powder) to obtain a gold luster on a polyimide film or glass substrate. This is achieved by the rubbing (in the parallel direction) and pressing (under a perpendicular force) of the oligomers to yield layer and tablet samples with gold tones, respectively. Importantly, the rubbing-based method employed herein does not involve crystallization, filtration, or dissolution, and therefore requires no use of special equipment, devices, or solvents. We also describe the relationship between gold tone development and molecular orientation (edge-on orientation *versus* face-on orientation), and special emphasis is placed on the fact that rubbing of the 3-methoxythiophene oligomer promotes the formation of edge-on lamellar crystallites in marked contrast to poly(3-alkylthiophene)s. Finally, the mechanism responsible for these processes is discussed.

2. Experimental

2.1. Materials

3-Methoxythiophene (>98%; Fujifilm Wako Pure Chemical Co.) was polymerized by oxidation with $Fe(ClO_4)_3 \cdot nH_2O$ (anhydrous salt content = 70.7%; Fujifilm Wako Pure Chemical Co.). Acetonitrile (>99.7%; Kanto Chemical Co., Ltd.), nitromethane (>98.0%; Tokyo Chemical Industry), and methanol (99.8%; Kanto Chemical Co., Ltd.) were used as received. Oligo(3-methoxythiophene) (O3MeOT) doped with ClO_4^- was prepared as previously reported.[17] More specifically, a solution of 3-methoxythiophene (0.123 g) in acetonitrile (10 mL) was placed in a glass cell and deaerated for 30 min by means of nitrogen gas bubbling through the solution while stirring at 350 rpm. This solution was instantaneously supplemented with a solution of $Fe(ClO_4)_3 \cdot nH_2O$ (1.10 g) in acetonitrile (10 mL), prepared by ultrasonication for 20 min. The resulting solution was stirred at 20 °C for 60 min and then suction-filtered through a membrane filter (pore size = 0.1 μm). The filter cake was washed vigorously with methanol at least three times, and the resulting powder was vacuum-dried at 50 °C for 1.5 h to yield ClO_4^--doped O3MeOT with a blackish-brown color. The molecular weight and perchlorate doping level of O3MeOT were 1.14×10^3 and 30%, respectively (see the literature 20 and its ESI). The glass plate (S1225, Matsunami Glass) was cleaned by sonication for 10 min in acetone (>99.5%; Kanto Chemical Co., Ltd.) prior to use.

2.2. Rubbing processing

Rubbing of the O3MeOT powder was performed in two ways, namely by applying a constant linear pressure (Method 1), and by applying a constant surface pressure (Method 2).

2.2.1. Method 1: application of a constant linear pressure.

Rubbing of the O3MeOT powder was performed using a home-made apparatus, as shown in Fig. 1. The substrate was fixed on a horizontally-moving aluminum stage, and the powder (95 mg) was placed on the substrate. The polyurethane rubber blade was fixed to jig A at a 45° angle to the substrate, and jig A was attached to the lifting device. A rubber blade was forced against the substrate using the elevating device. The pressure applied vertically to the substrate was converted to a voltage by a load cell (CLS-10NA, Tokyo Sokki Kenkyusho) attached to jig A, and was measured using an NR500 data logger and a high-speed analog voltmeter unit (NR-HA08, Keyence). Rubbing of the O3MeOT powder was performed by moving the stage back and forth in the horizontal direction, providing O3MeOT layers. The remaining powder was removed by means of air blowing. The linear pressures were 20 and 40 gf mm^{-1}, and the number of times that the stage was moved back and forth (*i.e.*, the number of rubbing cycles n) was either 10, 20, 50, or 100. A polyimide film containing dispersed carbon black was used as a substrate. This black film was employed as the substrate owing to the fact that the O3MeOT layer may exhibit low-saturation reflective colors due to the reflection of light from the substrate. The films were prepared by adding carbon black to a varnish containing a polyamic acid precursor (AH, Unitika) to prepare a coating solution, which was applied using a gap coater and then heated and baked to produce a carbon black-dispersed polyimide film with a thickness of 80 μm.

Rubbing was also performed at linear pressures other than 20 and 40 gf mm^{-1}. However, at linear pressures above 60 gf mm^{-1}, rubbing could not be performed due to high frictional forces. This may come from the increased linear contact area due to the elasticity of the urethane rubber blade. On the other hand, at linear pressures below 16 gf mm^{-1}, pressure could not be applied uniformly to the O3MeOT powder probably because uniform contact area cannot be achieved.

2.2.2. Method 2: application of a constant surface pressure.

The O3MeOT powder (200 mg) was placed at the center of a glass plate (76 mm × 52 mm) fixed to the stage, and the powder was covered by another glass plate of the same size. A glass plate with a size of 179 mm × 259 mm was then fixed on

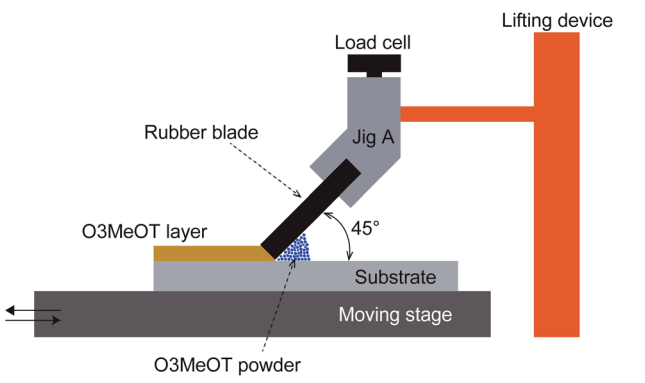

Fig. 1 Schematic illustration of the in-house-prepared equipment employed for the rubbing process according to Method 1.

that glass plate. Rubbing was then performed by placing a 5 kg weight on the top glass plate and moving the two top glass plates back and forth 50 times parallel to the stage. Subsequently, the remaining powder was removed by air blowing to obtain an O3MeOT layer. The area of the oligomer layer was measured and the surface pressure was calculated to be 282 gf cm^{-2} using the weight of the weight and glass plates.

2.3. Pressing procedure

The O3MeOT oligomer (100 mg) was placed in a stainless steel tablet molder (Shimadzu Corp.) and then pressed at 20 °C for 10 min using a hydraulic press (SSP-10A, Shimadzu Corp.) to produce tablets with a diameter of 13 mm. The applied pressure was varied from 0.05 t (3.8×10^{-2} tf cm^{-2}) to 10 t (7.5 tf cm^{-2}). For example, a sample pressed with a force of 2 t (1.5 tf cm^{-2} pressure) was denoted as tablet-2 t.

2.4. Characterization

The UV-vis reflection spectra of the obtained samples were recorded using a JASCO MSV-370 spectrometer, in which the incident and reflection angles were 23° from the vertical position. The spectra were recorded at 20 °C using an evaporated aluminum film, which was an accessory of the spectrometer, as the reference material. The O3MeOT layers were photographed using a digital microscope (VHX-5000, Keyence). The lustrous features of the films were demonstrated using optical micrographs. Illumination was performed using a ring-type lighting system attached to the microscope. While capturing the photographic images of the films, the distance between the light source and the sample, the illumination angle, and the photography angle were adjusted to almost constant values throughout. Out-of-plane X-ray diffraction (XRD) measurements were performed using a diffractometer (SmartLab, Rigaku) equipped with a Cu Kα ($\lambda = 1.5406$ Å) source in $2\theta/\omega$ scan mode. The colors of the layers and tablets were evaluated based on CIELab values acquired using a spectrophotometer (CM-600d, Konica Minolta) with a D65 illuminant at an observation angle of 10° (CIE 1964 Standard Observer); the parameters included a^* for redness–greenness and b^* for yellowness–blueness. The root mean square roughness values, R_q, of the O3MeOT layers were measured using laser-scanning microscopy (VK-9700, Keyence). The coating films were compared with a metallic gold film (thickness = 100 nm) on a glass plate, which was prepared by vacuum evaporation (VPC-260F, ULVAC).

3. Results and discussion

3.1. Rubbing of the O3MeOT powder

3.1.1. External appearance and surface roughness of the layer. While grinding the blackish-brown O3MeOT powder in an agate mortar for analysis purposes, we found that the ground powder developed a gold-like luster (see Fig. S1 in the ESI†). This finding motivated us to deal quantitatively with the gloss development induced by rubbing. Thus, Fig. 2 shows digital microscopy images of the O3MeOT layers obtained when the O3MeOT powder was rubbed with linear pressures of 40 and 20 gf mm^{-1} according to Method 1, wherein the rubbing direction corresponds with the up and down directions in the images. Low-magnification observations of the O3MeOT layers formed at 40 gf mm^{-1} (Fig. 2a–d) show a relatively highly lustrous gold tone, and the area occupied by the layer on the substrate increased with increasing values of n. In the high-magnification images (Fig. 2f–i), there was no powder-based granular morphology even at $n = 10$, indicating that the powder was crushed and spread out. In addition, smoothing of the layer surface was observed with increasing values of n. Indeed, when we measured the R_q values of the layers by laser microscopy, values of 1.6, 1.4, 1.2, and 0.99 were obtained for $n = 10$ (Fig. 2a and f), 20 (Fig. 2b and g), 50 (Fig. 2c and h), and 100 (Fig. 2d and i), respectively, which therefore confirm the above observation. As a reference, the value of R_q for the substrate (Fig. 2e) was also determined (*i.e.*, $R_q = 0.097$).

The area of the gold-like lustrous layer also increased with n for the layers formed at 20 gf mm^{-1}, but the areas were smaller than those prepared at 40 gf mm^{-1} using the same values of n (Fig. 2j–m). In the magnified images of these layers (Fig. 2n–q), the particle morphologies were remained regardless of n. However, as n was increased, the tops of the particles were squashed, and at $n = 50$ and 100, the squashed areas were connected to one another, leading to an increase in the lustrous area. Specular reflection spectroscopy and colorimetric measurements were therefore performed to quantify the gloss and chromaticity of each layer.

3.1.2. Optical properties of the O3MeOT layers. Fig. 3 shows the n dependence of the specular reflection spectra of the

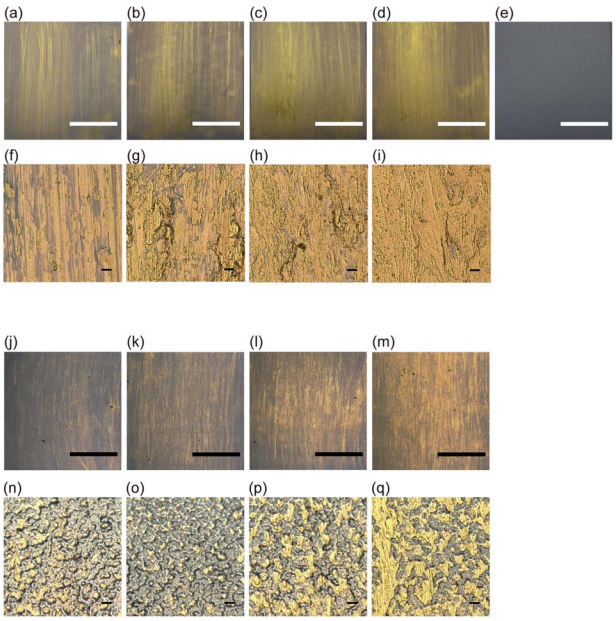

Fig. 2 Low-magnification (a–d, j–m) and high-magnification (f–i, n–q) digital microscope images of the O3MeOT layers prepared by rubbing at linear pressures of 40 (a–d, f–i) and 20 gf mm^{-1} (j–q). Panel (e) shows a low-magnification image of the substrate. The scale bars in the low-magnification images (a–e, j–m) and high-magnification images (f–i, n–q) correspond to 10 mm and 10 μm, respectively.

O3MeOT layers formed at 40 (Fig. 3a) and 20 gf mm^{-1} (Fig. 3b), wherein the reflection of the O3MeOT layers was mostly attributed to the yellow (570–590 nm), orange (590–620 nm), and red (620–750 nm) regions, with a slight green reflection (495–570 nm) also being present. The reflections in these wavelength regions are similar to the reflection characteristics of the metallic gold film, whose spectrum is also given in Fig. 3a. Consequently, the layers were characterized as possessing a gold hue. In addition, the reflection intensities were found to increase both with n and with the linear pressure, which indicates that the development of the gold tone is induced by a mechanochemical reaction. In addition, the a^*, b^* chromaticity diagram obtained for the layers prepared at 40 gf mm^{-1} (Fig. 3c) shows that the chromaticity of the oligomer powder is close to the origin (*i.e.*, close to black), and that the chromaticity of the O3MeOT layer approaches that of metallic gold with increasing values of n. On the other hand, when a linear pressure of 20 gf mm^{-1} was employed, the tendency of chromaticity to approach that of metallic gold with increasing values of n was retained (Fig. 3d); however, the extent of the increase was found to be relatively small. These colorimetric results are consistent with the results of the reflection spectral measurements. In our previous studies,[17–23] we found that two types of crystallites are present in the solution-cast films of O3MeOT, namely edge-on lamellar crystallites formed by the stacking of thiophene rings oriented perpendicular to the substrate (Fig. 4a), and face-on lamellar crystallites formed by the stacking of thiophene rings oriented parallel to the substrate (Fig. 4b); the edge-on lamellar crystallites were

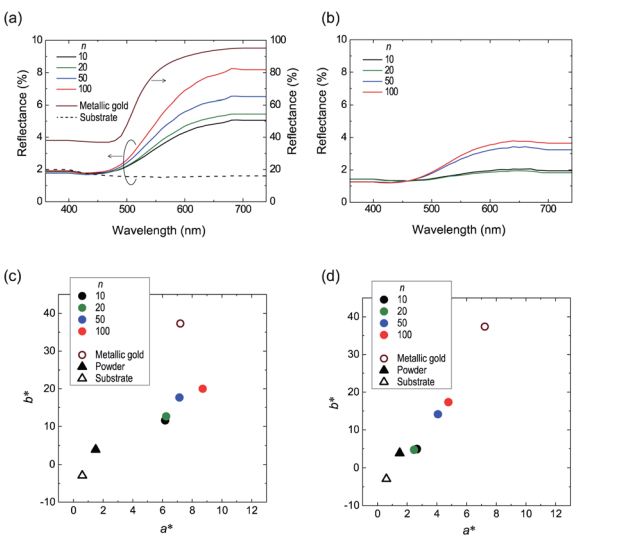

Fig. 3 Dependence of the specular reflection spectra of the O3MeOT layers prepared at linear pressures of (a) 40 and (b) 20 gf mm^{-1} on n. The corresponding spectra for the vacuum-evaporated gold film and the substrate are also shown for comparison. Panels (c) and (d) show the a^*, b^* chromaticity diagrams of the O3MeOT layers prepared at 40 and 20 gf mm^{-1} linear pressures, respectively. In addition to the data for the O3MeOT layers formed at $n = 10$, 20, 50 and 100, values for the O3MeOT powder, substrate, and vacuum-evaporated gold film are also included.

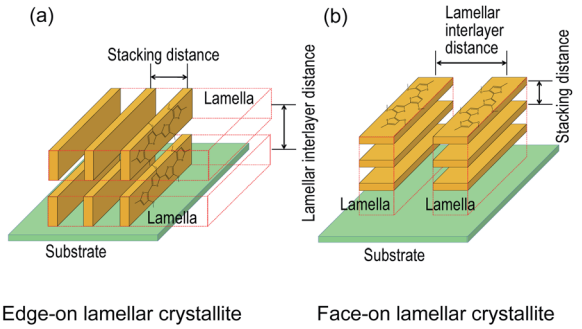

Fig. 4 Schematic diagrams of the (a) edge-on and (b) face-on lamellar crystallites.

dominant in these films. In addition, when the edge-on lamellae and face-on lamellae were observed from a direction perpendicular to the substrate, a gold tone and a low-gloss reddish-purple color were observed, respectively.[14] The colors of these two differently oriented lamellae are complementary to one another, thereby accounting for the blackish-brown color of the O3MeOT powder.[20] These experimental facts (Fig. 2 and 3) led us to assume that rubbing the powder parallel to the substrate changes the face-on lamellar orientation to the edge-on lamellar orientation, and increases the ratio of edge-on lamellar crystallites to face-on lamellar crystallites, thereby producing a gold-like luster. XRD measurements were therefore performed on the O3MeOT layers to confirm this assumption. However, it should be noted that the O3MeOT layers formed by Method 1 were too thin to be measured successfully, and thus, a relatively thick O3MeOT layer (hereafter abbreviated as O3MeOT layer 2) was prepared according to Method 2.

3.1.3. Optical properties and XRD measurements of O3MeOT layer 2. Fig. 5a shows a photographic image of O3MeOT layer 2. The average layer thickness was ~2 μm but varied widely, as shown in the image, and the value of R_q (2.1) was comparable to the layer thickness, thereby indicating a rough surface morphology. The specular reflection spectrum (solid red line in Fig. 5b) showed a higher reflection intensity compared to the spectra of Fig. 3a and b, and was comparable to the reflection intensity of the O3MeOT cast film (1.7 μm thick, R_q = 0.015) reported in our previous study[20] (dashed line in Fig. 5b). This implies that the ratio of reflection to absorption and transmission increases with the number of edge-on lamellar crystal layers in the film thickness direction, in addition to suggesting that the lamellar layers are responsible for light reflection. In the spectrum of O3MeOT layer 2, the wavelength corresponding to reflection rising edge (λ_r) was blue-shifted by 23 nm compared to λ_r = 487 nm for the cast film and metallic gold film. This was likely caused by the particularly large R_q value of O3MeOT layer 2, which causes the purple (380–450 nm), blue (450–495 nm), and green (495–570 nm) diffuse reflectance components to be added to the reflectance in the direction of the specular reflection. The contribution of this diffuse reflection imparted a whitish-gold tone to O3MeOT layer 2. Despite such an appearance, the chromaticity of O3MeOT layer 2 (solid red circle in Fig. 5c) was close to that of the

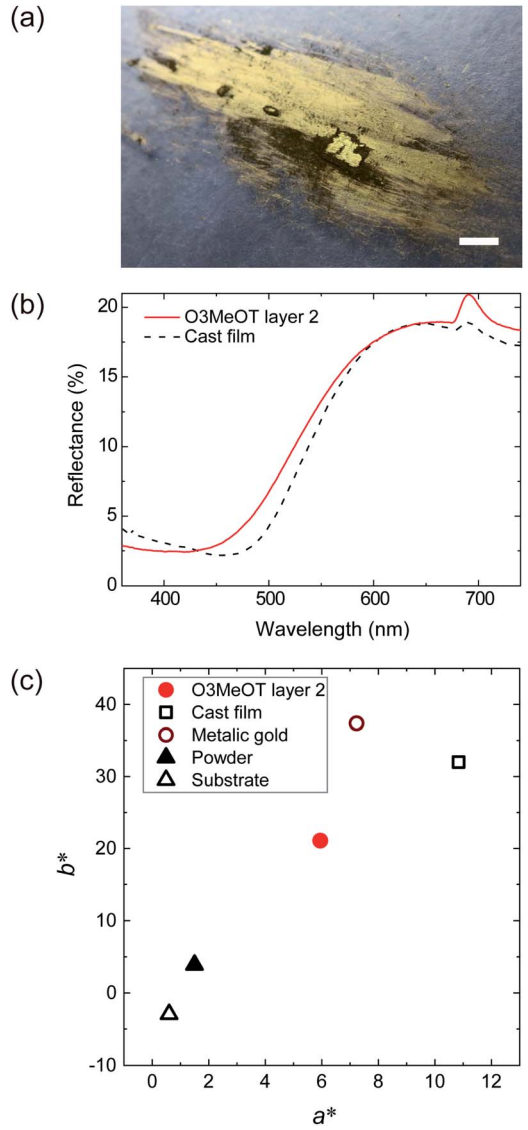

Fig. 5 (a) Digital microscopy image, (b) specular reflection spectrum (solid red line), and (c) a^*, b^* chromaticity diagram (solid red circles) of O3MeOT layer 2. The scale bar in panel (a) corresponds to 10 mm. For comparison, panel (b) includes the spectrum of a O3MeOT cast film, and panel (c) includes the colorimetric data for the cast film, metallic gold film, O3MeOT powder, and substrate.

O3MeOT layers ($n = 100$) shown in Fig. 3c and d. This indicates that the chromaticity of O3MeOT layer 2 itself is comparable to that of the O3MeOT layers; however, the diffuse reflection components in the purple to green regions are added to the specular reflection, resulting in a whitish appearance. In addition, variable-angle spectral reflectance measurements of O3MeOT layer 2 were performed, revealing that the gold-like luster of this layer did not originate from the structural color. Further details can be found in Fig. S3 and S4 in the ESI.†

Polyalkylthiophenes[37–41] and O3MeOT[17–19] are generally considered to be quasi-crystals comprising a crystalline area surrounded by an amorphous area, where the crystalline area consists of orthorhombic unit cells with lattice parameters of a, b, and c (Fig. 6b). Fig. 6a shows the XRD pattern (solid red line) of O3MeOT layer 2, and the corresponding patterns of the O3MeOT powder (solid black line) and the cast film (dashed line)[17] are also shown for comparison. The XRD pattern of the cast film was characterized by peaks at $2\theta = 7.84$, 15.92, and 25.46°, as previously reported.[17] The peaks at $2\theta = 7.84$ and 15.92° can be attributed to reflections from the crystallographic (100) and (200) planes, respectively, thereby confirming the lamellar structure of the film. The primary reflection at $2\theta = 7.84°$ was used to calculate the lamellar interlayer distance of 1.13 nm. Furthermore, the peak at $2\theta = 25.46°$ corresponds to the (020) plane, which is associated with the π–π stacking of the O3MeOT chains at a stacking distance of 0.35 nm. It should be noted here that the XRD measurements carried out herein were acquired in the out-of-plane mode and were therefore sensitive to the lattice parameters in the film thickness direction. Thus, the observation of signals at $2\theta = 7.84$ and 15.92° indicate the presence of edge-on lamellar crystallites (Fig. 4a), whereas the signal at $2\theta = 25.46°$ confirms the presence of face-on lamellar crystallites (Fig. 4b). Moreover, the reflection intensity from the (100) plane of the cast film was found to be significantly larger than that from the (020) plane, indicating that the edge-on lamellar crystals were dominant. The patterns of O3MeOT layer 2 and the O3MeOT powder both exhibited peaks at $2\theta = 7.87$, 16.03, and 26.03°, similar to the case of the cast films. However, the intensity ratios of the reflections from the (100) and (020) planes differed. More specifically, in the powder sample, the reflection from the (020) plane was slightly larger than that from the (100) plane, whereas for the O3MeOT layer 2 sample, the reflection intensity from the (100) plane was significantly larger. These observations clearly indicate that the

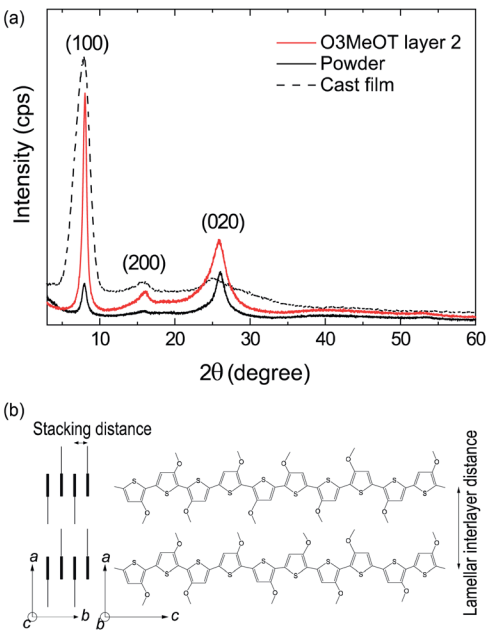

Fig. 6 (a) X-ray diffraction patterns of O3MeOT layer 2 (solid red line), the O3MeOT powder (solid black line), and the O3MeOT cast film (dashed line). (b) Schematic representation of the molecular arrangement of the O3MeOT oligomer.

rubbing action increased the edge-on lamellar structure, resulting in the development of a gold-like color and luster.

In films of poly(3-alkylthiophene)s (mainly poly(3-hexylthiophene), P3HT) and their derivatives, out-of-plane π–π stacking or face-on orientation is known to increase with mechanical rubbing;[24–30] this increase in the face-on component significantly improves hole transport in the out-of-plane direction. The above results for the O3MeOT layers and O3MeOT layer 2 also show orientation changes with rubbing, but the critical difference from the poly(3-alkylthiophene)s case is that the increase is not in the face-on orientation, but in the edge-on orientation, as shown in Fig. 3 and 6. This difference was likely caused by the difference between the alkyl and methoxy groups bonded to the 3-position of the thiophene ring. In the case of the alkyl groups, rubbing causes the alkyl chains with a low elastic modulus to elongate and align parallel to the rubbing direction, thereby enhancing the molecular planarity. These results therefore account for the ordering of such side-chain conformations to produce a greater proportion of face-on orientation crystallites.

On the other hand, in the case of a methoxy group, no elastic property is expected, and so orientation induction by the above mechanism is not expected to occur. Kim *et al.*[42] examined the interface between a P3HT film and an insulator substrate modified with self-assembled monolayers (SAMs) functionalized with various functional groups (–NH_2, –OH, and –CH_3). They found that a repulsive force exists between the non-covalent electron pairs of the terminal groups (–NH_2 and –OH) of the SAMs and the π-electron cloud of the thienyl backbone, leading to dominance of the edge-on orientation of P3HT. They further explained that when the terminal group of the SAM is –CH_3, the face-on orientation is dominant because of the π–H interaction between the H atom and the thienyl backbone. Based on their observations, it can be inferred that in the case of O3MeOT layer 2, the edge-on orientation is the most thermodynamically stable because of the repulsive force between the thienyl skeleton and the unshared electron pairs of the –OH groups present on the glass substrate (or –C═O on the polyimide film for the O3MeOT layers).[43]

3.2. Pressing of the O3MeOT powder

During a previous study, we wished to perform Fourier transform infrared spectroscopy measurements on O3MeOT, and so we sandwiched the O3MeOT powder between two dies and pressed it. Surprisingly, we found that a gold-like luster had developed. This motivated us to further examine luster development under pressing conditions. For this purpose, tablets were prepared by pressing O3MeOT powder using the method described in Section 2.3, and their material properties were measured. Fig. 7 shows photographs of the obtained tablets, while Table 1 lists their thicknesses and R_q values. Visually, as the applied pressure increased, the color of the tablet surface was observed to gradually change from blackish-brown (*i.e.*, the color of the powder) to a gold tone. As described in Section 2.4, the photographic conditions for each tablet were as much as possible the same: however, the reproduction of the gold tone luster by photographing is very difficult and may differ from the visual images. For the quantitative evaluation of luster, see the results of the reflection spectrum measurements shown below.

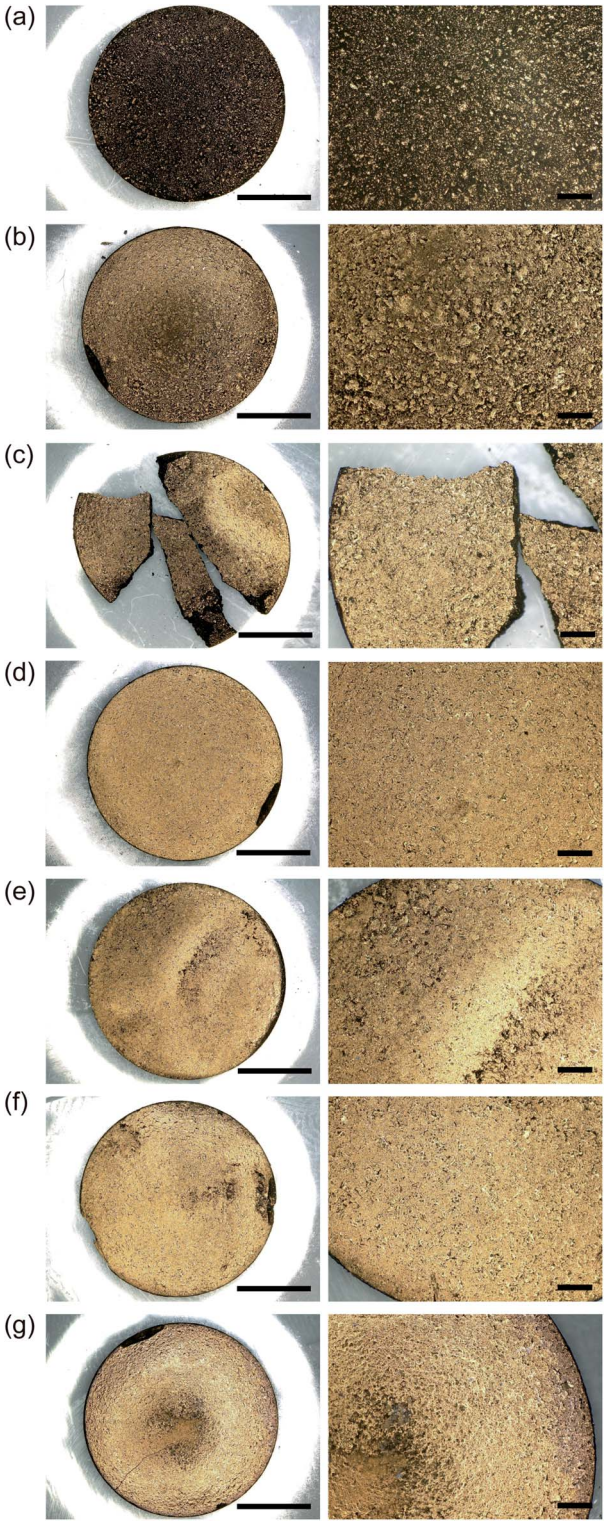

Fig. 7 Digital microscopy images of (a) tablet-0.05 t, (b) tablet-0.5 t, (c) tablet-1 t, (d) tablet-2 t, (e) tablet-4 t, (f) tablet-8 t, and (g) tablet-10 t. The left- and right-hand images in each panel are the images taken at low and high magnifications, respectively. The scale bars in the left- and right-hand images correspond to 5 and 1 mm, respectively.

Table 1 Thickness and R_q values of tablet samples

Tablet sample	Thickness (mm)	R_q
Tablet-0.05 t	0.95	26.3
Tablet-0.5 t	0.75	8.3
Tablet-1 t	0.70	8.0
Tablet-2 t	0.65	3.4
Tablet-4 t	0.60	3.7
Tablet-8 t	0.65	2.7
Tablet-10 t	0.55	1.3

In addition, the tablet thickness and the R_q value decreased with increasing pressure.

Notably, the chipped parts of the tablet surface (Fig. 7b, d, and g), the fracture surface at the broken part of the tablet bulk (Fig. 7c), and the cross sections of the bulk of all tablets remained blackish-brown, and only the surface developed a gold luster. See Fig. S2 in the ESI† for the laser microscopy images of the surface topography of the tablets.

Fig. 8a shows the reflection spectra of the tablets, wherein it can be seen that the spectral shape obtained for the tablet sample was comparable to those of the cast film and the metallic gold film (Fig. 3a), thereby indicating that their reflective color is a gold tone. In addition, we found that the specular reflectance was positively correlated with the applied pressure. Furthermore, in the a^* and b^* chromaticity diagrams of the tablets (Fig. 8b), as the applied pressure was increased, the chromaticity of the powder tended to gradually approach that of the cast film. By analogy with the luster development observed by rubbing (Section 3.1), the development of a gold luster under pressing led us to assume that the number of edge-on lamellae increased in the tablets under these conditions. To confirm this assumption, we performed XRD measurement using the tablet-10 t sample (Fig. 9).

The obtained patterns show peaks at $2\theta = 7.81$, 15.75, and 25.81°, corresponding to reflections from the (100), (200), and (020) planes, respectively. The positions of these peaks were nearly identical to those of the O3MeOT layer 2 and O3MeOT powder patterns shown in Fig. 6. However, the area ratio γ of the (100) peak to the (020) peak differed from sample to sample. More specifically, γ increased in the order: powder ($\gamma = 0.34$) < tablet-10 t ($\gamma = 0.56$) < O3MeOT layer 2 ($\gamma = 1.01$) < cast film ($\gamma = 9.15$). This order is almost identical to that of the maximum reflectance values observed for their corresponding reflection spectra (see Fig. 5b and 8a), indicating that the ratio of edge-on lamellae to face-on lamellae is one of the factors that determines the extent of the luster. However, in tablet-10 t, the increased proportion of edge-on lamellae is likely to be limited to the vicinity of the tablet surface, since the tablet bulk had the same color as the powder, as previously described. Therefore, its value of γ (*i.e.*, 0.56) was only slightly larger than the corresponding value for the powder (*i.e.*, 0.34) owing to the fact that the crystal structures detected in the XRD analysis are likely to contain a substantial contribution from the tablet bulk. Furthermore, it was found that the (100) peaks of O3MeOT layer 2 and tablet-10 t have full widths at half-depths of 0.57° and 1.04°, respectively, indicating that the former has a larger crystallite size in the out-of-plane direction. The above results therefore indicate that rubbing is superior to pressing as

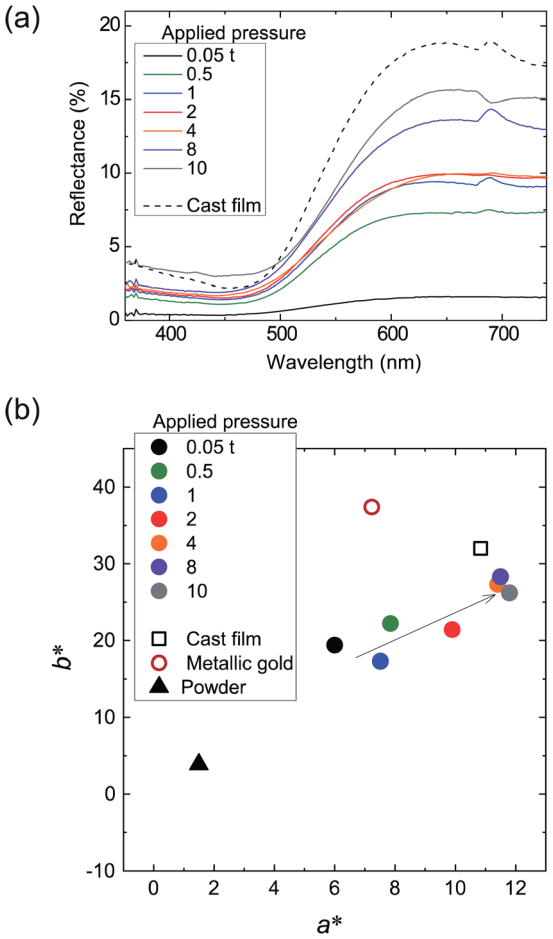

Fig. 8 (a) Specular reflection spectra of tablet-0.05 t, tablet-0.5 t, tablet-1 t, tablet-2 t, tablet-4 t, tablet-8 t, and tablet-10 t. The reflection spectrum of a cast film is also included for comparison. (b) a^*, b^* chromaticity diagrams for the above tablet samples shown with the chromaticities of the cast film, vacuum-evaporated gold film, and O3MeOT powder for comparison.

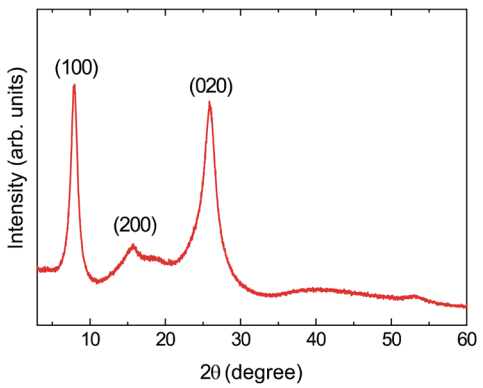

Fig. 9 X-ray diffraction pattern of tablet-10 t.

a method of producing lusters in terms of a smaller applied pressure, a larger value of γ, and the formation of larger edge-on lamellar crystallites.

Notably, in the tablet samples, the development of the gold tone luster was limited to the near-surface area, even though the same pressure was applied to the tablet bulk and its surface.

It has been previously reported that the surface of the stainless steel die, which is a component of the tablet mold, is covered with a passive film bearing hydroxide residues and bonded water.[44–46] Thus, based on the polyalkylthiophene orientation model[42] presented by Kim *et al.*, it would be expected that the amount of edge-on lamellae increases close to the die/tablet interface owing to the repulsion between the species having unshared electron pairs (hydroxide residues and bonded water) and the thienyl backbone. However, this repulsion is limited to the interface and does not extend to the tablet bulk, and so the bulk exhibits the same orientation properties as the powder. To confirm this mechanism, it will be necessary to modify the die surface with alkyl groups and investigate whether the face-on orientation becomes dominant close to the tablet surface.

4. Conclusions

In this study, it was found that rubbing or pressing the blackish-brown 3-methoxythiophene oligomer powder produced layers or tablets with a gold-tone color. During rubbing, the application of a higher pressure perpendicular to the powder and the use of an increased number of rubbing cycles resulted in a higher specular reflectance for the obtained layers, and the chromaticity of the resulting layer approached that of metallic gold. X-ray diffraction (XRD) analysis of the layer indicated that rubbing increased the ratio (γ) of edge-on to face-on lamellar crystallites, wherein the former is responsible for the development of the gold-like luster. Although the widely studied rubbing effect for poly(3-alkylthiophene)s results in a face-on lamellar dominance due to the alkyl group orientation effect, this differed from the oligo(3-methoxythiophene) system investigated herein, which contains no alkyl group. More specifically, in this case, the main interaction is the electronic repulsive force between the substrate functional group with unshared electron pairs and the π-electron cloud of the thienyl backbone. Based on this mechanistic model, we assumed that the increase in γ with rubbing was induced by the repulsive force.

Furthermore, during the pressing process, an increase in the applied pressure was found to result in a higher specular reflectance for the resulting tablet, and its chromaticity approached that of metallic gold. XRD analysis showed that pressing also increased the value of γ; however, the development of the gold tone was limited to the tablet surface, and the bulk remained blackish brown, *i.e.*, the color of the original powder. We therefore assumed that the existence of repulsive forces between the thienyl skeleton and the unshared electron pairs on the stainless die surface used in the pressing process may be limited to the die/tablet interface and may not extend into the tablet bulk. As a result, the formation of edge-on lamellar crystallites was not induced beyond the surface, and the corresponding gold-like luster failed to develop beyond the surface. Based on our results, the rubbing process shows potential for application in the field of gold-tone decoration because it produces a substantial number of edge-on lamellar crystallites despite the low applied pressure and does not require any special equipment. The rubbing effect observed for oligo(3-methoxythiophene), *i.e.*, the edge-on orientation effect, is therefore expected to contribute to the development of new organic electronics. Future studies will focus on the effect of the chemical composition of the rubbing substrate on the molecular orientations of the resulting layers.

Author contributions

Satoya Sugiura: conceptualization, data curation, formal analysis, investigation, writing – original draft; Terumasa Mitogawa: data curation, investigation, visualization; Kota Saito: data curation, investigation; Rihito Tamura: data curation, investigation; Satoru Tsukada: data curation, writing – review & editing; Takahiko Horiuchi: data curation, formal analysis; Katsuyoshi Hoshino: conceptualization, funding acquisition, project administration, supervision, writing – original draft.

Conflicts of interest

There are no conflicts to declare.

Acknowledgements

This work was financially supported by the JSPS KAKENHI (Grant 20K05614 to K. H.). The authors thank the Center for Analytical Instrumentation of Chiba University for the XRD and reflectance measurements.

References

1 F. J. Maile, G. Pfaff and P. Reynders, *Prog. Org. Coat.*, 2005, **54**, 150–163.
2 H. Liu, H. Ye and Y. Zhang, *Colloids Surf., A*, 2008, **315**, 1–6.
3 K. Ogura, R. Zhao, H. Yanai, K. Maeda, R. Tozawa, S. Matsumoto and M. Akazome, *Bull. Chem. Soc. Jpn.*, 2002, **75**, 2359–2370.
4 R. Zhao, M. Akazome, S. Matsumoto and K. Ogura, *Tetrahedron*, 2002, **2**, 10225–10231.
5 R. Zhao, S. Matsumoto, M. Akazome and K. Ogura, *Tetrahedron*, 2002, **58**, 10233–10241.
6 K. Ogura, R. Zhao, M. Jiang, M. Akazome, S. Matsumoto and K. Yamaguchi, *Tetrahedron Lett.*, 2003, **44**, 3595–3598.
7 K. Ogura, R. Zhao, T. Mizuoka, M. Akazome and S. Matsumoto, *Org. Biomol. Chem.*, 2003, **1**, 3845–3850.
8 K. Ogura, K. Ooshima, M. Akazome and S. Matsumoto, *Tetrahedron*, 2006, **62**, 2484–2491.
9 A. Matsumoto, M. Kawaharazuka, Y. Takahashi, N. Yoshino, T. Kawai and Y. Kondo, *J. Oleo Sci.*, 2010, **59**, 151–156.
10 K. Kondo, A. Matsumoto, K. Fukuyasu, K. Nakajima and Y. Takahashi, *Langmuir*, 2014, **30**, 4422–4426.

11 N. Saito, M. Ono, H. Komatsubara, K. Fukushima, Y. Takahashi and Y. Kondo, *Dyes Pigm.*, 2020, **179**, 108394.
12 Y. Kojima, K. Kishikawa, S. Ichikawa, J. Matsui, K. Hirai, Y. Kondo and M. Kohri, *ACS Appl. Polym. Mater.*, 2021, **3**, 1819–1827.
13 H. Goto, *J. Polym. Sci., Part A: Polym. Chem.*, 2013, **51**, 3097–3102.
14 T. Tokuda and K. Hoshino, *Polym. J.*, 2016, **48**, 1141–1149.
15 H. Takada, T. Ochiai and M. Nagata, *Thin Solid Films*, 2019, **677**, 33–38.
16 D. Takamura and K. Hoshino, *Chem. Lett.*, 2018, **47**, 540–543.
17 R. Tagawa, H. Masu, T. Itoh and K. Hoshino, *RSC Adv.*, 2014, **4**, 24053–24058.
18 Y. Takashina, T. Mitogawa, K. Saito and K. Hoshino, *Langmuir*, 2018, **34**, 3049–3057.
19 Y. Takashina and K. Hoshino, *Polym. J.*, 2019, **51**, 591–599.
20 M. Tachiki, R. Tagawa and K. Hoshino, *ACS Omega*, 2020, **5**, 24379–24388.
21 M. Tachiki, S. Tsukada and K. Hoshino, *Dyes Pigm.*, 2021, **190**, 109302.
22 M. Kubo, H. Doi, R. Saito, K. Horikoshi, S. Tsukada and K. Hoshino, *Polym. J.*, 2021, **53**, 1019–1029.
23 M. Kubo, M. Tachiki, T. Mitogawa, K. Saito, R. Saito, S. Tsukada, T. Horiuchi and K. Hoshino, *Coatings*, 2021, **11**, 861.
24 M. Brinkmann, L. Hartmann, L. Biniek, K. Tremel and N. Kayunkid, *Macromol. Rapid Commun.*, 2014, **35**, 9–26.
25 W. A. Memon, Y. Zhang, J. Zhang, Y. Yan, Y. Wang and Z. Wei, *Macromol. Rapid Commun.*, DOI: **10.1002/marc.202100931**.
26 R. Zhu, A. Kumar and Y. Yang, *Adv. Mater.*, 2011, **23**, 4193–4198.
27 L. Hartmann, K. Tremel, S. Uttiya, E. Crossland, S. Ludwigs, N. Kayunkid, C. Vergnat and M. Brinkmann, *Adv. Funct. Mater.*, 2011, **21**, 4047–4057.
28 V. Vohra, G. Arrighetti, L. Barba, K. Higashimine, W. Porzio and H. Murata, *J. Phys. Chem. Lett.*, 2012, **3**, 1820–1823.
29 D. Kajiya, S. Ozawa, T. Koganezawa and K. Saitow, *J. Phys. Chem. C*, 2015, **119**, 7987–7995.
30 D. Kajiya, T. Koganezawa and K. Saitow, *J. Phys. Chem. C*, 2016, **120**, 23351–23357.
31 J.-C. Wittmann and P. Smith, *Nature*, 1991, **352**, 414–417.
32 M. Misaki, Y. Ueda, S. Nagamatsu, M. Chikamatsu, Y. Yoshida, R. Azumi, N. Tanigaki and K. Yase, *Appl. Phys. Lett.*, 2005, **87**, 243503.
33 N. Tanigaki, S. Nagamatsu, W. Takashima and Y. Yoshida, *Thin Solid Films*, 2009, **518**, 853–856.
34 H. Sirringhaus, P. J. Brown, R. H. Friend, M. M. Nielsen, K. Bechgaard, B. M. W. Langeveld-Voss, A. J. H. Spiering, R. A. J. Janssen, E. W. Meijer, P. Herwig and D. M. de Leeuw, *Nature*, 1999, **401**, 685–688.
35 L. Biniek, N. Leclerc, T. Heiser, R. Bechara and M. Brinkmann, *Macromolecules*, 2013, **46**, 4014–4023.
36 V. Untilova, J. Hynynen, A. I. Hofmann, D. Scheunemann, Y. Zhang, S. Barlow, M. Kemerink, S. R. Marder, L. Biniek, C. Müller and M. Brinkmann, *Macromolecules*, 2020, **53**, 6314–6321.
37 M. J. Winokur, P. Wamsley, J. Moulton, P. Smith and A. J. Heeger, *Macromolecules*, 1991, **24**, 3812–3815.
38 T. J. Prosa, M. J. Winokur, J. Moulton, P. Smith and A. J. Heeger, *Macromolecules*, 1992, **25**, 4364–4372.
39 R. D. McCullough, S. Tristram-Nagle, S. P. Williams, R. D. Lowe and M. Jayaraman, *J. Am. Chem. Soc.*, 1993, **115**, 4910–4911.
40 K. E. Aasmundtveit, E. J. Samuelsen, M. Guldstein, C. Steinsland, O. Flornes, C. Fagermo, T. M. Seeberg, L. A. A. Pettersson, O. Inganäs, R. Feidenhans'l and S. Ferrer, *Macromolecules*, 2000, **33**, 3120–3127.
41 Y. Qu, L. Li, G. Lu, X. Zhou, Q. Su, W. Xu, S. Li, J. Zhang and X. Yang, *Polym. Chem.*, 2012, **3**, 3301–3307.
42 D. H. Kim, Y. D. Park, Y. Jang, H. Yang, Y. H. Kim, J. I. Han, D. G. Moon, S. Park, T. Chang, C. Chang, M. Joo, C. Y. Ryu and K. Cho, *Adv. Funct. Mater.*, 2005, **15**, 77–82.
43 Y. Nakamura, Y. Suzuki and Y. Watanabe, *Thin Solid Films*, 1996, **290–291**, 367–369.
44 G. Okamoto, *Corros. Sci.*, 1973, **13**, 471–489.
45 J. Ruijing, W. Yuwu, W. Xu, C. Changfeng and Z. Jingmao, *Appl. Surf. Sci.*, 2017, **412**, 214–222.
46 G. Okamoto and T. Shibata, *Nature*, 1965, **208**, 1350.